



Optimal Red Mud Replacement Level Evaluation in Conventional Concrete Based on Fresh and Hardened Concrete Characteristics

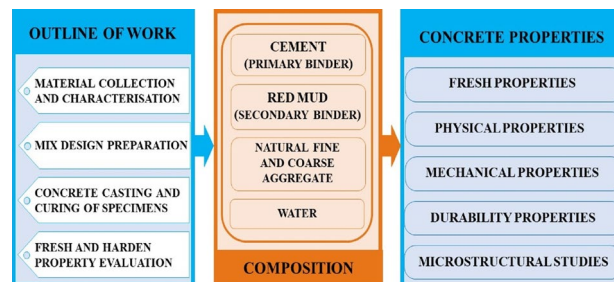
Soumyaranjan Panda¹ · Monalin Pradhan¹ · Saubhagya Kumar Panigrahi¹

Received: 24 January 2024 / Accepted: 22 April 2024 / Published online: 6 May 2024
© The Minerals, Metals & Materials Society 2024

Abstract

The global annual industrial waste production is enormous, influencing the environmental parameters affecting the whole universe. Due to rapid industrialization, cement production is increasing to meet the demand of the construction industries, harming the atmosphere and prompting scarcity of natural resources. Thus, the need for a supplementary cementitious material is essential, replacing cement either partially or completely. In the current investigation, red mud, which has some cementitious and hydraulic characteristics, is being utilized as a supplementary cementitious material and is used as a partial replacement to cement in concrete production at different percentage levels like 0% (the control concrete), 5%, 10%, 15%, 20%, and 25% with an intension to establish the optimal replacement level established on various fresh and hardened concrete characteristics. All workable mixes are subjected to physical tests (density measurement), mechanical tests (ultrasonic pulse velocity test, rebound hammer test, compressive and tensile strength test), and durability tests (acid resistance test, sulfate resistance test, and chloride resistance test). The discussions on the concrete characterization variations can be substantiated through various microstructure level tests like scanning electron microscopy (SEM), energy-dispersive X-ray spectroscopy (EDX), and X-ray diffraction analysis (XRD) tests. The detailed characterization tests mutually confirmed that the optimal red mud replacement level in conventional concrete is evaluated to be 15%, leading to a sustainable production evolving reasonable waste management.

Graphical Abstract



Keywords Red Mud · Supplementary cementitious materials · Mechanical properties · Durability properties · Microstructural analysis

Introduction

Concrete, which is also known as artificial stone, has significantly contributed to the development of infrastructure. To fulfill the demand for urban development and industrial growth around the globe, the construction industry has grown very fast, enhancing the use of cement concrete [1].

The contributing editor for this article was Hiromichi Takebe.

✉ Saubhagya Kumar Panigrahi
skpanigrahi_ce@vssut.ac.in

¹ Department of Civil Engineering, VSSUT Burla, Sambalpur, Odisha 768018, India

Cement production involves the heating of limestone and clay using fossil fuels. Calcination of limestone and combustion of fossil fuel releases CO₂. As per the data available, each ton of Portland cement production releases 0.94 tons of CO₂. Cement industries are responsible for the emission of 8–9% of total CO₂ emissions globally [2]. The emission of CO₂ results in environmental concerns like global warming, acidification, and eutrophication [3, 4]. The energy used for the production of cement is another concern; for each ton of Portland cement, 80-kilowatt-hour power is needed, which is 2–3% of global energy consumption [5].

In contrast, globally, a significant amount of industrial waste is generated, and natural resources are running out. India produces over 290 million tons of inorganic industrial waste each year [6, 7]. The primary causes of environmental contamination are the accumulated solid wastes and their annual growth. These wastes appear to be particularly difficult to handle, transport, and dispose of. The use of these industrial wastes as a suitable binding material component in the construction industries can overcome the aforementioned problems because of sustainability [8, 9].

Industrial wastes from a variety of industries, such as red mud (RM), fly ash, copper slag, silica fume, powdered granulated blast furnace slag, natural rock minerals, and so on, are easily accessible for use as supplementary cementitious material (SCM) [10–14]. RM is a bauxite residue left as a byproduct during alumina manufacturing [15, 16]. More than 300 million tons of red mud are produced worldwide each year by the alumina industries. For each ton of alumina produced, more than one ton of red mud is discharged [17, 18]. Several authors [19–21] have noticed that RM has cementitious qualities, but the accurate limit of percentage replacement has not been found yet.

In the current investigation, ordinary Portland cement (OPC) is partially replaced by RM, which is a supplementary cementitious material. Using fresh, physical, mechanical, durability, and microstructural examinations, the impacts of RM substitution are examined to determine the optimal replacement level.

Research Significance

The incorporation of SCM not only enhances eco-friendliness but also mitigates the Portland cement demand. Despite numerous studies affirming the suitability of RM, a byproduct from the bauxite industry, as an SCM, the quest for an optimized proportion in conventional concrete remains elusive [22–24]. The absence of a comprehensive study on concrete properties concerning RM utilization from a specific source introduces ambiguity in determining its ideal dosage. This knowledge gap poses a challenge in harnessing the full potential of RM as an SCM, hindering its seamless integration into mainstream construction practices. This ongoing

investigation undertakes a meticulous examination of conventional concrete properties, focusing on the partial substitution of RM across varying percentages. Encompassing a comprehensive spectrum, the study meticulously evaluates workability, physical characteristics, mechanical attributes through both non-destructive and destructive tests, durability attributes under chemical attacks, and microstructural characteristics. The exhaustive study not only identifies an optimized mix composition but also provides a future slope to the researchers for further studies.

Materials

OPC of grade 43 manufactured by Ultratech cement confirming IS:8112-1989 [25] was used to produce conventional concrete, regarded as the control mix. The OPC used was free from lumps, powdery, and had appropriate rheological behavior [26]. The cement was substituted by RM, an SCM, at various replacement percentage levels to prepare further concrete mixes collected from NALCO, Damanjodi plant, Odisha. Since RM was used as the SCM, its physical characteristics were determined as per the procedures adopted to test the cement's physical characteristics. The chemical composition (evaluated through X-ray fluorescence, XRF) and physical properties of both binders, OPC and RM, are shown in Table 1 and Table 2. To perform XRF, finely ground (< 75 μm) OPC and RM samples were collected. The sample elemental composition is determined in a non-destructive manner, using an XRF spectrometer, Malvern Panalytical Epsilon 4, with 135 eV resolution (Mn-Kα) and having 1 ppm as the lower limit of detection. The binder samples were finely ground ensuring their homogeneity for precise results. The loose powder samples were pressed to form pallets and placed in a spectrometer for the XRF test. The locally available natural coarse aggregates (NCA) and natural fine aggregates (NFA) under saturated surface dry (SSD) conditions were used for the preparation of the concrete mix. The aggregates characterization test results were

Table 1 Oxide composition of OPC and RM through XRF

Oxide components of OPC	Percentage present	Oxide components of RM	Percentage present
SiO ₂	21.5	SiO ₂	14.8
Al ₂ O ₃	4.0	Al ₂ O ₃	21.2
Fe ₂ O ₃	3.5	Fe ₂ O ₃	44.1
CaO	63	CaO	3.7
SO ₃	2.5	Na ₂ O	6.8
MgO	2	TiO ₂	2.96
LOI	2.3	LOI	0.72

Table 2 Physical characteristics OPC and RM with adopted standards

Properties	OPC results	RM results	Code followed
Specific gravity	3.13	3.15	IS: 4031 (part 11)-1988 [29]
Fineness (%)	5	2.65	IS: 4031 (part 1)-1996 [30]
Consistency (%)	32	38	IS: 4031 (part 4)-1988[31]
Initial setting time (min)	50	60	IS: 4031 (part 5)-1999 [32]
Final setting time (min)	295	325	IS: 4031 (part 5)-1999 [32]
Soundness (mm)	3	–	IS: 4031 (part 5)-1999 [32]

carried out confirming Indian standard code IS 2386–1963 (Part-1 and 3) [27, 28] and are shown in online supplementary material Table S-1. The gradation curves of both NFA and NCA are shown in Fig. S-1. Clean tap water was used in accomplishing the concrete mix.

RM is finer than cement particles. The consistency and setting time test imply that, with the increase in the RM content, the water demand increases. Both the initial and final setting time is also more than the reference cement. This is due to more fine particles being available in RM and, thus, requiring more water than cement. The setting time in RM is more because of the slow hydration in the early stage. The specific gravity of RM is similar to that of cement, and there is no apparent volume expansion in the case of RM.

Mix Proportions

Six different mixes were developed to examine the effect of red mud through cement replacement on conventional concrete. In this work, mix designs were prepared as per the guidelines of IS 10262: 2019 [33]. Cement concrete RM00, the control mix, was prepared in the proportion of 1:1.675:2.98 (cement: NFA: NCA) by weight. Five cement-substituted mixes by RM have been created to determine the ideal replacement percentage to be evaluated through fresh, mechanical, durability, and microstructural studies with a comparison to the OPC-based control mix [34, 35]. The mixes RM05, RM10, RM15, RM20, and RM25 have red mud replacement percentages of 5%, 10%, 15%, 20%, and 25%, respectively, by weight of cement. For all mixes, the water/ cement (w/c) ratio was kept constant at 0.5. Various

mixes were executed through weigh batching. The detailed mix designs in the current study are presented in Table 3.

Preparation, Casting, and Curing of Specimens

Following the proper mix design (“**Mix Proportions**” Section) with characterized materials (“**Materials**” Section), all the mixes, as in Table 3, were prepared. To get complete concrete characterization involving fresh, mechanical, durability, and microstructural properties, cubes along cylinders of sizes 150 × 150 × 150 mm and 150 mm diameter with 300 mm height were cast. Each mix required eighteen number cubes and nine cylinders (detail explained in “**Testing Methodology**” Section) with the mentioned dimensions prepared. The mold was cleaned and greased before casting [36, 37]. After 24 h of casting, prepared specimens were demolded and kept under water curing for the required age of curing. The detailed procedure is given in Fig. 1.

Testing Methodology

After detailed material characterization as discussed in “**Materials**” Section, the concrete mix design was prepared (“**Mix Proportions**” Section), and concrete specimens (cubes and cylinders) were cast (“**Preparation, Casting, and Curing of Specimens**” Section) to determine the hardened concrete properties (mechanical, durability, and microstructural properties) following due-specified curing period of 7 day, 28 days, and 90 days, depending on the requirement. The

Table 3 Mix proportions of all six control and blended binder-based concrete

Mix ID	% RM	Cement (kg/m ³)	RM (kg/m ³)	NFA (kg/m ³)	NCA (kg/m ³)	Water (kg/m ³)
RM00	0	387	00	648.4	1152	193.5
RM05	5	367.65	19.35	648.4	1152	193.5
RM10	10	348.3	38.7	648.4	1152	193.5
RM15	15	328.95	58.05	648.4	1152	193.5
RM20	20	309.6	77.4	648.4	1152	193.5
RM25	25	290.25	96.75	648.4	1152	193.5

RM red mud, NFA natural fine aggregate, NCA natural coarse aggregate



Fig. 1 General preparation procedure of concrete mixes

fresh characteristics were evaluated after the concrete was prepared, i.e., before concrete casting. The current section provides a full explanation of the experimental approach to all mentioned tests.

Fresh Concrete Characteristics

The slump cone test, which is the frequently accepted test not for very wet or very dry concrete, was adopted (Fig. S-2) to assess the workability performance of the freshly prepared concrete following Indian Standard IS 1199–1959 [38] and SP 23: 1982 [39]. The acceptable range of concrete slump tests for different concrete types to understand their workability is presented in Table 4.

Mechanical Properties: Hardened Concrete Characteristics

The short-term performance of concrete is evaluated using mechanical tests consisting of non-destructive tests (NDT) like ultrasonic pulse velocity (UPV) test to evaluate the concrete quality, rebound hammer (RH) test to predict the

compressive strength without crushing the concrete sample, and destructive tests (DT) like unconfined compressive test and split tensile test to evaluate the concrete compressive strength (CS) and split tensile strength (STS).

Non-Destructive Tests (NDT): Mechanical Testing

To evaluate the concrete's flaws without demolishing, non-destructive testing is performed on concrete samples [40]. The UPV method is an NDT technique used to determine the homogeneity of the concrete sample. It was carried out following IS 13311 (part 1): 1992 [41]. The UPV test equipment comprises two transducers: transmitter and receiver. The transmitter sends out an ultrasonic pulse, which gets received by the receiver. The ultrasonic pulse velocity is determined based on the distance between the transmitter and the receiver and is used to evaluate concrete quality by detecting the presence of any concrete irregularity like fracture, fissures, etc., due to several causes, such as non-uniform mixing, internal crack growth, and environmental or chemical influences. Table 5 provides information regarding the concrete quality based on UPV value according to IS 13311 (part 1): 1992 [41]. The results of the rebound hammer (RH) test, which was carried out following IS 13311(Part 2):1992 [42], represent the surface hardness or compressive strength of the outer concrete layer with a thickness of 30–50 mm [43]. The RH test operates on the concept that the rebound extent is expressed through a rebound number of an elastic mass striking a concrete surface, characterizing its surface's hardness. The rebound number is correlated with the compressive strength through a graph plotted on the instrument surface. The spring-pulled mass rebounds when the rebound hammer's plunger is pressed against the concrete surface and subsequently released. The RH test is performed on the concrete surface layer and is thus seen as an 'indicator' of concrete strength. Although there is no clear relationship between concrete strength and hardness, however, IS 13311(Part 2):1992 [42] guideline indicates that predicted CS from RH test must lie within $\pm 25\%$ of destructive CS. In the NDT experimentation, instruments like GILSON CT-133 and Proceq Original Schmidt were used for the UPV and RH tests, respectively. The UPV and RH tests are shown in Fig. S-3(a) and (b). The cube specimens (150 × 150 × 150 mm) were used for both the NDT tests.

Table 4 Concrete type based on ranges of slump value (SP 23:1982)

Concrete type	Degree of workability	Slump range (mm)
Stiff	Very low	0–25
Stiff plastic	Low	25–50
Plastic	Medium	75–100
Flowing	High	150–175

Table 5 Specified concrete quality based on the UPV value

Pulse velocity (km/s.)	Quality of concrete
$UPV \geq 4.5$	Excellent
$3.5 \leq UPV < 4.5$	Good
$3.0 \leq UPV < 3.5$	Medium
$UPV < 3.0$	Doubtful

Destructive Tests (DT): Mechanical Testing

The concrete CS test and STS tests were carried out as per IS 516: 1959 [44] and IS 5816: 1959 [45] using the compression testing machine (CTM) with a constant load per minute, i.e., 14N/mm^2 (or 140 kg/cm^2) per minute and $1.8\text{ N/mm}^2/\text{minute}$, respectively. The cube samples ($150 \times 150 \times 150\text{ mm}$) and cylindrical samples (150 mm diameter with 300 mm height) were utilized for the evaluation of CS and STS, respectively. To prevent any inaccurate test results, each of the results was declared based on the average of three specimen test results [46]. To establish a continuous periodic check in the process of target strength attainment, each of the destructive tests was carried out at 7 days, 28 days, and 90 days of the curing period. The CS and STS tests are shown in Fig. S-3(c) and (d).

Durability Properties: Hardened Concrete Characteristics

Workable, strong (short-term characteristics) concrete should be durable (long-term characteristics), i.e., the concrete strength must not deteriorate significantly, impeding its structural expectations as every structure has a pre-defined structural life. Among all durability issues, a concrete structure majorly deteriorates because of environmental chemical attacks [47]. Thus, in the current study, concrete specimens were subjected to various chemical resistance tests, i.e., acid resistance test, sulfate resistance test, and chloride resistance test. All the tests were carried out with 28 days of cured concrete specimens, and in each test, the average results of three cubes were declared as the corresponding durability test result.

Acid Resistance Test: A Durability Test

Concrete structures are subjected to a variety of acidic conditions, including sewage, industrial wastewater, acid rain, and microbiological acid attack. A highly soluble calcium salt is created as a byproduct in an acid reaction with the calcium hydroxide component of cement paste, which results in an acid attack [48]. The dissolution of the calcium silicate hydrate can cause major structural damage to concrete in the most severe acid assault scenario. Loss of weight and CS are two common means to estimate the acid degradation extent. The test was conducted following ASTM C1898 (2020) [49]. The cube specimens were immersed in a 3% H_2SO_4 solution for 90 days.

Sulfate Resistance Test: A Durability Test

There exist two possible explanations for sulfate attack: endogenous (non-environmental) and exogenous

(environmental). Sulfate ions, which have been found in large quantities in the soil, groundwater, ocean, decaying organic matter, and industrial wastewater, are transferred into the concrete, affecting its strength development mechanism. The effect of sulfate attack on the concrete durability was studied by performing the sulfate resistance test [50]. The extent of sulfate degradation is generally expressed through weight loss and CS loss. To investigate the concrete sulfate resistance, specimens were immersed in a 3% MgSO_4 solution for 90 days.

Chloride Attack: A Durability Test

The concrete matrix chloride ion permeability promotes corrosion characteristics. Therefore, to examine the chloride resistance of concrete, a solution of sodium chloride (NaCl) was prepared in which 3% by weight of sodium chloride was mixed with ordinary potable water. The specimens were immersed for 90 days to evaluate the chloride penetration depth. The test was performed as per ASTM C1218 (2020) [51].

Microstructural Analysis: Hardened Concrete Characteristics

The observations in the short-term and long-term characteristic study can also be resonated through different microstructural analyses. Microstructural investigations help us to understand the material behavior at the microscopic level. It provides information about the compositional morphology, the chemical elements and functional groups present, the mass loss caused by the heat application, and the existence of sample minerals. Three tests have been carried out for the microstructural analysis which was described in the current section. All the tests were carried out with 28 days of cured concrete specimens.

Scanning Electron Microscopy (SEM): A Microstructural Test

The Hitachi SU3500 instrument was employed for SEM analysis. Following the destructive unconfined compressive strength test, a small portion was removed from the concrete cube's core and placed inside the chamber for which SEM analysis was performed on the fractured concrete samples, and secondary electron (SE) images were acquired. SEM examination employing SE images reveals morphological characteristics of the material. This study uses electron energy of 10 kV to generate SE pictures of $\times 500$ magnification and $100\text{ }\mu\text{m}$ resolution. The SEM analysis adhered to ASTM C1723-16 [52].

Energy-Dispersive X-ray Spectroscopy (EDX): A Microstructural Test

The SEM and EDX tests were conducted on the same instrument. Hitachi SU3500 is additionally supplied with a Bruker XFlash 6–10 EDX detector for obtaining atomic composition data. The same sample (as in SEM) was used for EDX detection. Although major elements can achieve a precision of $\pm 1\%$, overall analytical accuracy is typically around $\pm 2\%$ due to uncertainties in standard compositions and errors in corrections applied to raw data. The EDX test was carried out following ASTM E1508-12a guidelines [53].

X-ray Diffraction (XRD) Analysis: A Microstructural Test

XRD analysis was executed using a PANalytical Xpert PRO powder diffractometer, performing at 35 kV with Cu- $K\alpha$ radiation (2θ) within the range 20° to 80° and Ni filler ($\lambda = 1.5418 \text{ \AA}$) with step size of 0.03° , having scan step time of 0.6 s. Concrete samples have been extracted from the matrix's inner core and a small sample piece was powdered to a fine $90 \mu\text{m}$. The sample was then oven-dried for 24 h. It was then applied to a glass slide with a smooth surface, placed in a sample holder, and distributed with double-stick tape. The XRD equipment produces a diffraction pattern, which can be analyzed to determine the mineral phases present in the concrete. The experimentation was carried out following ASTM C1365-18 [54]. The XRD spectra of concrete mixes were analyzed using X'pert HighScore software, supported by the Powder Diffraction File (PDF) database of the International Centre for Diffraction Data (ICDD).

Result and Discussion

The concrete sample specimens prepared (“[Preparation, Casting, and Curing of Specimens](#)” Section) were tested for complete characterization as per the techniques mentioned (“[Testing Methodology](#)” Section). The detailed observations from all the characterizing tests under workability, mechanical, durability, and microstructural analysis, along with the complete reasoning, are furnished in the current section.

Fresh and Physical Characterization Test Results

The fresh characteristics, i.e., mix workability of all mentioned concrete mixes (Table 3), are established through the slump cone test. The test results are shown in Table 6.

The concrete's slump measurement was executed by calculating the distance between the top of the cone-filled concrete and the top of the slumped concrete cone. To carry out all the proposed mechanical and durability characteristics, concrete under each mix was batched and mixed thrice. The fresh slump value was determined thrice in all three batches for each mix. The slump results among all three attempts in each mix vary within a 5% coefficient of standard deviation (SD). The results reveal that the control mix lies in the ‘medium’ workability range as per IS 10262: 2019 [33], i.e., within 50–100 mm. The RM substitution in the mix causes a gradual reduction in the workability (Table 6). However, for RM substitution till 15%, though there is a gradual reduction in the slump value, still the slump value lies in the same ‘medium’ range. Further RM substitution (RM20, RM25) is found to have lower workability and lie in the ‘low’ workability range (25–50 mm). Finely ground red mud (Table 2) increases the mix's surface area, demanding more water for adequate wetting and particle lubrication, reducing available water for maintaining workability (slump) in concrete mixes, thus workability reduces [55].

Physical property is evaluated through the density measurement of the concrete mix. After 28 days of curing, the density of each specimen was calculated, and the results are presented in Table 6. It is observed that the control mix has a density of 2389 kg/m^3 . The RM-substituted mixes exhibit higher density than the control mix. Hence, with an increase in RM content, the concrete density is enhanced because the RM finer particle (Table 2) fills the voids of the mix. In each mix, concrete density was determined with the average results of three cube specimens. The evaluated coefficient of SD is less than 15%.

It can be concluded from the fresh and physical characterization that with an increase in RM content in the conventional concrete mix, the workability gradually reduces, and the density continuously increases. However, RM replacement up to 15% is optimal as the reduced workability lies in the same range as the control concrete.

Mechanical Characterization Test Results

The mechanical property of concrete mixes is evaluated through both NDT (UPV, RH) and DT (CS, STS). Result interpretations, along with necessary discussions, are presented in the current section.

Table 6 Slump and density values of all concrete mixes

Mix	RM00	RM05	RM10	RM15	RM20	RM25
Slump value (mm)	78	65	55	50	41	33
Density (kg/m^3)	2389	2400	2412	2427	2446	2459

Non-Destructive Test Results: A Mechanical Test Results Interpretation

Concrete homogeneity defects in concrete, like cracks and voids, were examined through the UPV test. Table 7 shows the UPV and RH test results of all mixes at 28 days of curing. The results show that the control mix has ‘excellent’ concrete quality (>4.5 km/s). Out of all five RM-substituted mixes, up to 15% RM replacement, i.e., RM05, RM10, and RM15 mixes, also lie in the excellent category (Table 7). However, at a higher replacement percentage, i.e., RM20 and RM25, concrete is in the ‘good’ category (3.5–4.5 km/s). RM at a higher proportion level (RM20, RM25) may increase the water demand, reducing the w/b (water to binder) ratio, leading to concrete quality degradation [56]. Predicted RH compressive strength results are listed in Table 7. The RH results signify that the RM increment reduces the predicted CS compared to the conventional concrete. RM being a byproduct of aluminum refining has inherent characteristics like iron and aluminum-rich chemical composition, high alkalinity, etc., which may limit its effectiveness as a direct replacement for cement because of setting time, hydraulic reactivity, and strength development [57]. The UPV and RH results declared are the average of three and twelve data values, respectively, according to Indian standards. NDT values provide a very precise outcome with a minimal SD of 5%.

Destructive Test Results: A Mechanical Test Results Interpretation

The concrete compressive strength through the cubical specimens was determined at the curing age of 7, 28, and 90 days from casting. The test results of all mixes are presented in Table 8. At each age of curing, the strength results declared with average outcomes of three specimens. The SD

is determined based on the deviation of the result from the average value. The destructive mechanical strength results of all the mix combinations lie within a 15% coefficient of SD, which is in the allowable range as per IS 516: 1959 [44] guidelines. It can be observed that at all curing ages, the concrete CS mostly got reduced with the rise in the RM replacement level due to the lower hydraulic activity of RM. There is an initial CS reduction in RM05; further, it increases marginally till RM15, and then the strength rapidly decreases in both 28 and 90-day cured samples. At 15% RM replacement level, the CS is approximately similar to that of control concrete. In the 5% to 15% range, the presence of pozzolanic materials in RM reacts with calcium hydroxide that enhances compressive strength marginally by promoting the formation of C–S–H, C–A–H, and C–A–F–H gels [58]. Beyond 15%, higher RM content can increase water demand, negatively impacting the w/b ratio. Elevated water demand can lead to insufficient cement hydration, resulting in CS reduction [59]. It is clear from Table 8 that the strength of all the RM-blended concrete in the 7-day curing period is lower than the control mix. At an early age, the strength gain of concrete containing a higher percentage of RM is found to be less because of the presence of a lower amount of C_2S and C_3S [60]. On enhancing the curing duration, the strength increases gradually. Figure 2 represents the CS of all mixes at different curing periods. Both for 28-day and 90-day cured concrete, the strength reduction in RM-blended concrete concerning control conventional concrete is 9%, 7%, 6%, 21%, 30%, and 12%, 11%, 8%, 19%, and 23% at 5%, 10%, 15%, 20%, and 25% RM replacement levels. It can be observed that though the CS change patterns are the same, for 28-day cured samples, the CS reduction to the 15% replacement level is smaller, and beyond 15%, the CS reduction is higher for those 90-day cured samples. Thus, it shows at a higher curing level, the RM-blended mixes exhibit a higher rate of CS reduction. In the initial curing

Table 7 UPV and RH test results for all concrete mixes (non-destructive testing)

Mix	RM00	RM05	RM10	RM15	RM20	RM25
UPV (km/s)	4.551	4.513	4.521	4.523	4.465	4.352
RH (MPa)	29.12	25.54	28.26	27.84	25.29	21.62

Table 8 CS and STS test results of all concrete mixes at various curing periods (destructive testing)

Mix	Compressive strength (CS)			Split tensile strength (STS)		
	7 days	28 days	90 days	7 days	28 days	90 days
RM00	28.46	34.86	38.09	2.27	2.77	2.97
RM05	26.44	31.56	33.35	2.05	2.18	2.41
RM10	25.79	32.25	33.93	2.13	2.53	2.64
RM15	23.88	32.81	34.96	2.11	2.48	2.59
RM20	22.15	27.51	30.99	1.14	1.62	1.83
RM25	20.03	24.27	29.21	1.04	1.32	1.53

Fig. 2 CS and STS result variation pattern of all concrete mixes at different curing periods

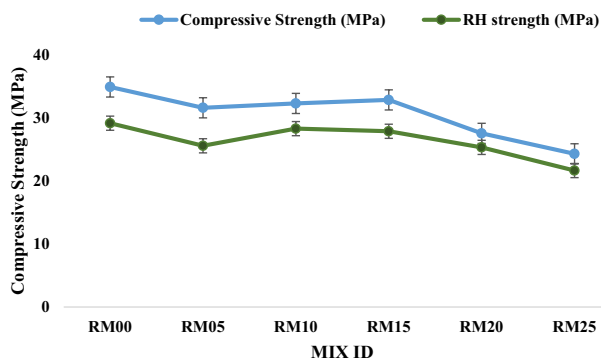
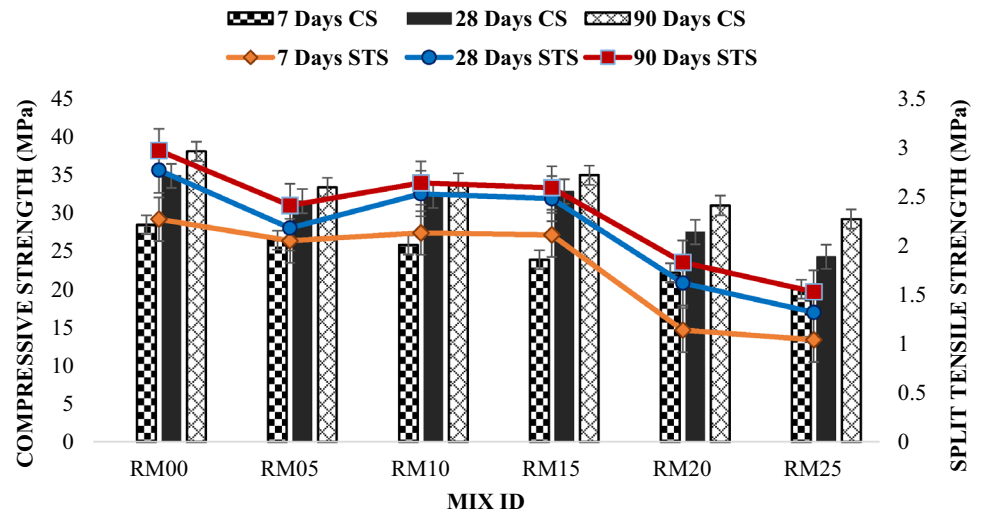


Fig. 3 Comparative results presentation between CS (destructive) and predicted RH (NDT)

period (28 days), the pozzolanic activity might lead to a rapid increase in CS. Despite the initial strength gain, the 5% to 15% replacement levels experience a more pronounced dilution effect over the extended curing period, which results in lesser strength gain [60]. Figure 3 shows the graphical representation between destructive CS and strength prediction from the RH test. The graph signifies that RH results lie $\pm 25\%$ of destructive CS, which satisfies the standard codal provisions.

The split tensile strength (STS) of the concrete samples is determined at 7 days, 28 days, and 90 days of curing periods. The STS results are provided in Table 8 and are graphically demonstrated in Fig. 2. It can be observed that the STS of all the RM-blended mixes at all the curing periods are lower than that of the respective control mixes. Under each curing period and among all RM-blended mixes, the STS attains a maximum value of RM10, which is very close to the value of RM15. Beyond RM15, the STS reduced further. As in reinforced concrete structures, the tensile strength of concrete is negligibly small; thus, without much difficulty, the cement can be replaced with the RM. The STS in RM15 is reduced

by 7%, 10%, and 12% to the respective control mixes at 7 days, 28 days, and 90 days of curing periods. Further, it is noticed that similar to CS, at a higher curing period, the RM-blended mixes exhibit a higher rate of strength reduction.

Critical Discussions on Mechanical Characterization

The mechanical characterization is performed through both NDT and DT tests. The mechanical characteristics of the control conventional mix are superior to those of RM-blended mixes. Though the concrete quality of the control mix is similar to that of RM-blended mixes up to 15%, from remaining mechanical characterization tests, it can be concluded that RM15 is the optimal blended mix, providing maximum mechanical strength among all blended mixes and having acceptable strength reduction concerning the control mix. A higher curing period causes a higher rate of strength reduction in RM-blended mixes. The NDT-RH test results lie within $\pm 25\%$ of the DT-CS results.

Durability Characterization Test Results

The durability characterization test results performed in the current manuscript demonstrate the concrete chemical resistance. The results of acid resistance, sulfate resistance, and chloride resistance are discussed in the current sections. In all these durability tests, the average result of three specimens was considered. The SD of results lies within 10% of the acceptable range.

Acid Resistance Test: A Durability Test Results Interpretation

Concrete is subjected to various environmental issues that can hinder its durability characteristics. Test results are expressed through the percentage of weight loss and strength loss at 90 days of acid immersion. Various mixes under acid

immersion with the corresponding concrete weight loss percentage along with strength loss percentage are represented in Fig. 4. A higher percentage of weight loss and strength loss is noticed in control concrete specimens (RM00) than in each RM-blended mix justifying RM-mixes performed better durability concerning acid resistance to the conventional concrete. Among five RM-mixes, the weight loss gets continuously reduced from RM05 to RM25; however, from RM05 to RM15, the weight loss reduction is quite gradual, and from RM15 to RM25, a higher reduction is noticed. This observation can be interpreted as among RM05 to RM15; the weight reduction is stabilized, justifying that RM15 is the critical one. Within the 5% to 15% replacement range, the pozzolanic reaction products enhance the density and chemical stability of the concrete, making it more resistant to acid attack. Among five RM-mixes, the strength loss gets reduced continuously from RM05 to RM15, and beyond, it gets enhanced, justifying RM15 as the most preferred mix concerning both strength loss and weight loss. The alkalinity of the RM accelerates the C–S–H gel formation. The higher alkaline nature of RM leads to concrete matrix densification. The excessive red mud content can potentially cause pore refinement or pore blocking, bringing about a continuous reduction in weight loss percentage [59]. Acid attack on concrete primarily occurs through the dissolution of calcium-based compounds (e.g., calcium hydroxide) in the cement paste matrix. However, at higher RM content (beyond RM15) the decreased porosity may limit the diffusion of calcium hydroxide and other calcium-based compounds necessary for neutralizing acids, responsible for a greater strength loss. Thus, RM content increase influenced the acid attack capacity, exhibiting poor concrete resistance.

Sulfate Resistance Test: A Durability Test Results Interpretation

The sulfate resistance test results of all the mixes at 90 days of immersion in 3% magnesium sulfate solution are shown

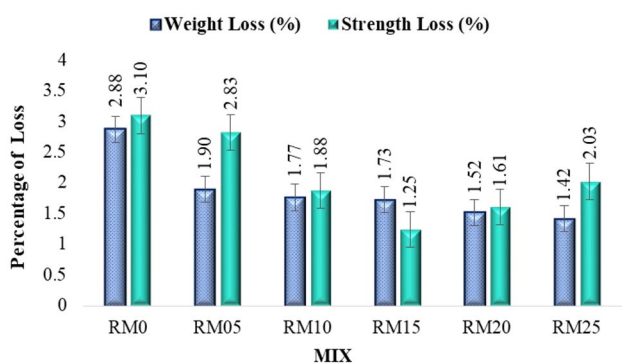


Fig. 4 Variation in percentage weight and strength loss among different concrete mixes in acid resistance test

in Fig. 5, representing percentage weight and strength losses against different concrete mixes (RM00 to RM25). A continuous reduction in both weight loss and strength loss can be noticed with an increase in the RM content. Thus, the sulfate resistance increases with RM content, and the RM-blended mixes are more durable concerning sulfate resistance to conventional concrete. The enhancement of RM as cementitious components may lead to the formation of sulfate-resistant compounds, such as ettringite and other stable hydrates inside concrete. These compounds contribute to the concrete’s ability to resist sulfate attack [61].

Chloride Attack: A Durability Test Results Interpretation

To know the relation between RM replacement percentages along with the depth of chloride ion penetration inside concrete cubes on immersing in NaCl solution, experimentation was performed as per “Chloride Attack: A Durability Test” Section, and results are presented in Fig. 6. The RM particles are finer than cement particles (Table 2), with an increase in the RM content, the concrete density gets enhanced (Table 6)

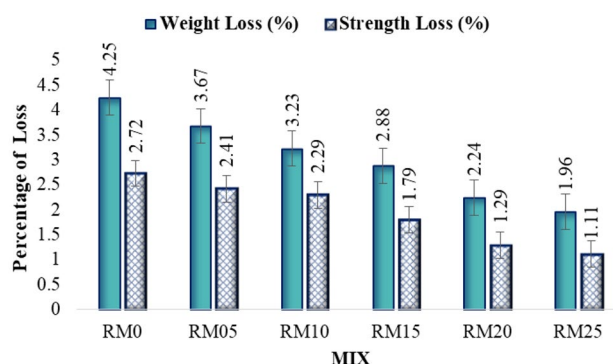


Fig. 5 Variation in percentage weight and strength loss among different concrete mixes in sulfate resistance test

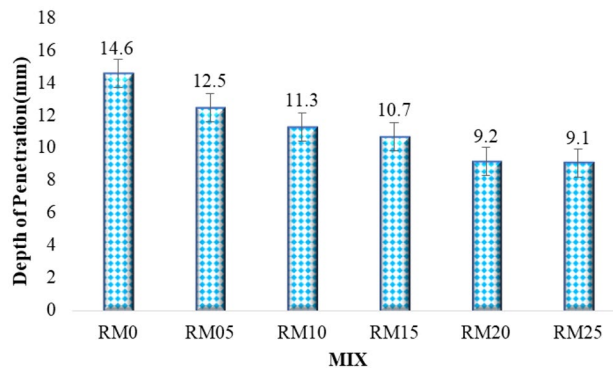


Fig. 6 Variation in chloride ion penetration inside concrete in different concrete mixes in chloride attack test

resulting diminished porous structure and permeability. It is also substantiated through Fig. 6 that the depth of chloride ion penetration reduced with the increase in RM content. The least penetration occurred with RM25. The RM-blended mixes are superior to the conventional concrete concerning the chloride attack. It is worth mentioning that on the penetration of chloride ions inside concrete structures, the reinforcement gets corroded, and a preferable solution is the use of RM-blended mix than conventional mix.

Statistical Analysis

Through a statistical test tool ANOVA (Analysis of Variance), the statistical significance of durability studies was examined. The mean values of the reported acid and sulfate attack outcomes from the experimental data were taken into account. The ANOVA test was run with a significance level of 0.05. The dependent variable in the analysis is the percentage of weight loss and strength loss in concrete with varying amounts of red mud, ranging from 0 to 25%. The results were reported as statistically significant because the ANOVA outcomes (Table 9) show that the P value is less than 0.05. Multiple comparison analysis was performed using the Tukey [honestly significant differences (HSD)] test to analyze the average durability outcomes of RM-blended concrete mixes.

Where,

SS = Sum of squares due to the source

df = Degrees of freedom in the source

MS = Mean sum of squares due to the source

F = F-statistic

F crit = F-critical

Tukey Criterion was followed by the equation $T = q \sqrt{(MSE/n_i)}$

Where,

$q_{\alpha(c, n-c)}$ = Studentized range distribution based on c and $n-c$ degree of freedom

• C = Number of treatments

• n = Total sample size

MSE = Mean square error

n_i = Sample size of the treatment group with the smallest number of observations.

The absolute values of the paired means show that, according to the T value, there is no significant difference

in the strength loss resulting from sulfate and acid attack (T value $> |X_i - X_j|$ mean). However, a significant difference occurred in the weight loss of the concrete samples as a result of these durability tests (T value $< |X_i - X_j|$ mean).

Critical Discussions on Durability Characterization

The durability characteristics study in the current manuscript demonstrates the concrete chemical resistance, including acid resistance, sulfate resistance, and chloride resistance. The durability study can be summarized as follows. The RM-blended mixes are more durable than conventional concrete in all three chemical resistance tests. The optimal RM replacement level is evaluated to be 15% from the acid resistance test. However, on enhancing the RM replacement level beyond 15%, the RM-blended concrete becomes more resistant in both sulfate and chloride resistance tests.

Microstructural Analysis Test Results

In the current section, results of the microstructural analysis, i.e., SEM, EDX, and XRD tests (conducted as per “[Microstructural Analysis: Hardened Concrete Characteristics](#)” Section) on all the mix samples are discussed.

Scanning Electron Microscopy (SEM): A Microstructural Test Results Interpretation

The SEM microstructural analysis for all six mixes was performed as per “[Scanning Electron Microscopy \(SEM\): A Microstructural Test](#)” Section to check the morphological development at 28 days of curing. As blended concrete is a heterogeneous material, the hydration products confer the formation of random microstructural views. The microstructure of the concrete sample is based on some parameters like elements present in the base materials, duration or stages of the hydration, the physical appearance of the hydrates, total quantity of reacted materials, unreacted materials, morphological transformation, etc. The prime hydration products of the blended concrete are tobermorite (C–S–H), portlandite (CH), quartz (SiO₂), calcite, and ettringite. Some unreacted elements of the base material can be noticed through the microstructural analysis.

The SEM analysis images of the control and RM-blended concrete samples are shown in Fig. 7a–f. In the control concrete (Fig. 7a), the production of the C–S–H phase is

Table 9 ANOVA outcomes for durability tests

Source of variation	SS	df	MS	F	P value	F crit
Between groups	5.293754	3	1.764585	3.624521	0.030815	3.098391
Within groups	9.736924	20	0.486846			
Total	15.03068	23				

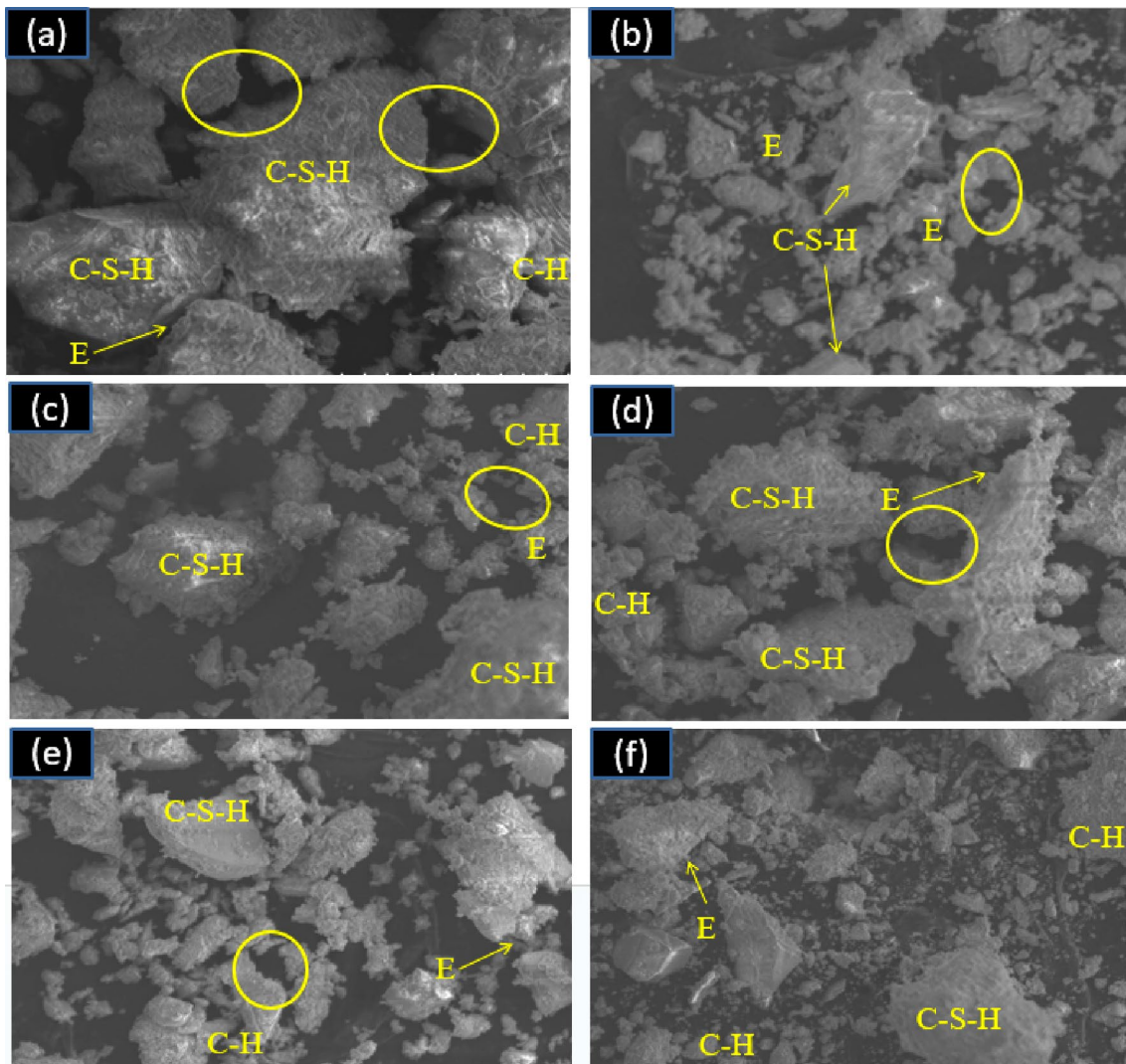


Fig. 7 SEM images for different mixes **a** RM00; **b** RM05; **c** RM10; **d** RM15; **e** RM20; **f** RM25

observed with small needles and crystal-like structures. A very small amount of the plate-shaped image is available, showing less quantity of CH phase. Few pores can be noticed with black stains (encircled portions). On replacing cement with RM at various proportions, a comparatively dense microstructure can be obtained.

In the SEM images of RM05 (Fig. 7b), some ettringite (E) with a needle-like structure can be noticed, which is advantageous for the structural density. Certain anhydrides like RM can be noticed with bright, narrow plate-like structures. The increase in RM content produces a dense structure, which may be due to the less pore structure in the RM with well spreads and blends in the cement mortar paste. Some needle-like and compact crystalline structures (showing the C–S–H gel available) are noticed in the RM15 mix (Fig. 7d). In addition, some solid form of the CH phase is available, showing a small plate-like structure. RM15 has a similar

SEM image to the control mix, which also provides nearly similar strength results. In the blended cement mortar paste with 25% RM replacement, a non-homogeneous structure along with unreacted RM can be noticed (Fig. 7f), which may be due to the high RM content in the cement mortar paste. Thus, more ettringites (due to more Al) are formed, affecting the structure and the concrete strength. Therefore, high RM content results in lower strength gain. The above discussion agrees on the fact that the RM 15% replacement mix is the most preferred one among all blended mixes.

Energy-Dispersive X-ray Spectroscopy (EDX): A Microstructural Test Results Interpretation

The EDX of the concrete sample was conducted as per “Energy-Dispersive X-ray Spectroscopy (EDX): A Microstructural Test” Section to quantify the available elements

in the paste. Figure 8 provides information regarding the elemental composition of all six mixes. The EDX test analysis results of all concrete mixes are presented in Table 10.

The existence of Si, Ca, and O in all these samples suggests the likely development of calcium silicate hydrate (C–S–H) gel as the main reaction product. The quantity of alumina gradually increases with higher RM content. It

is further noticed that in RM-blended mixes, Fe traces are also noticed (RM05–RM25). The presence of higher Al and Fe content (RM10 and RM15) contributes to the formation of other cementitious compounds, such as calcium aluminate hydrate (C–A–H) and calcium aluminoferrite hydrate (C–A–F–H), that are helpful for overall strength development [58]. On further RM content enhancement (RM20 and

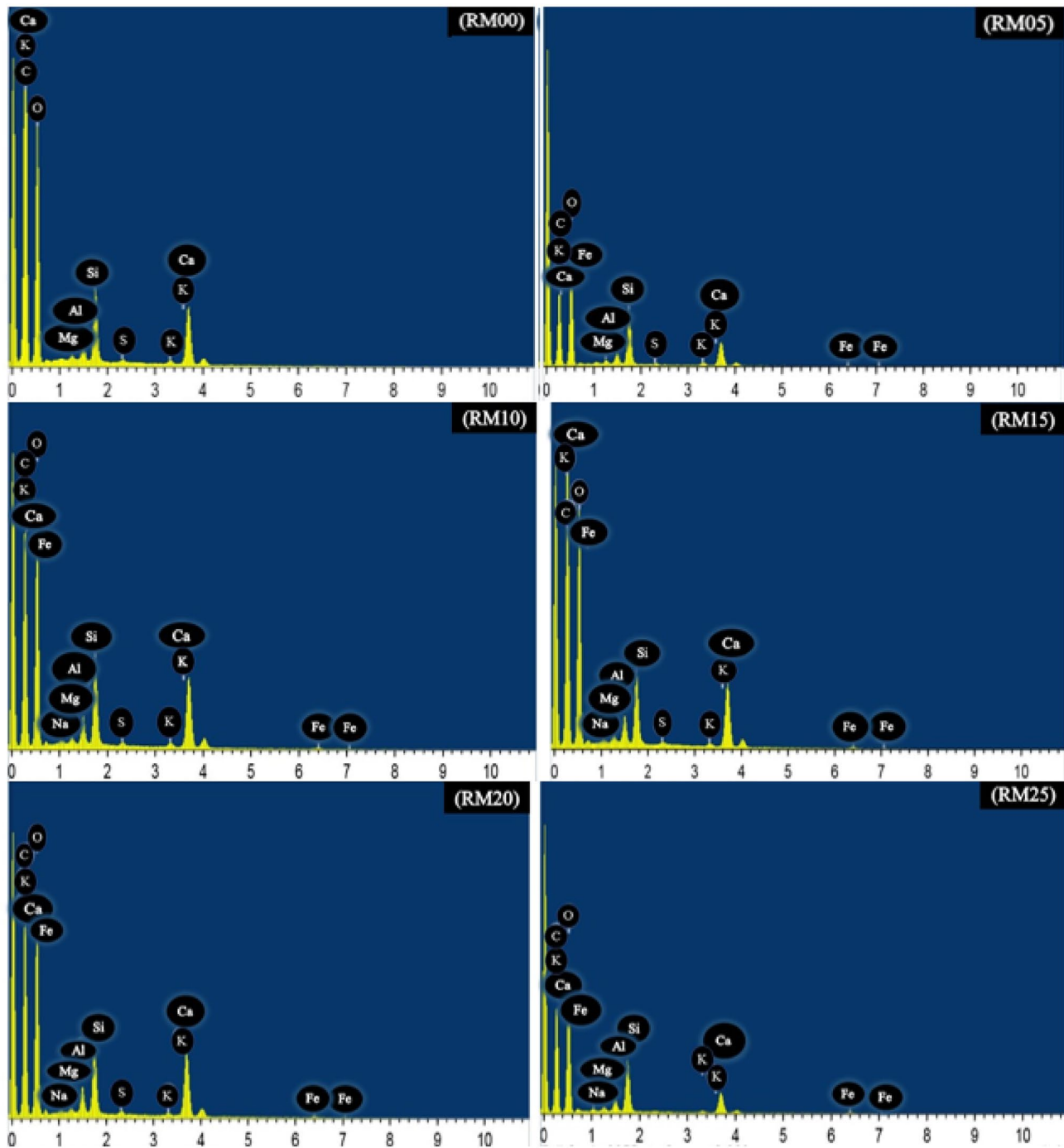


Fig. 8 EDX test results for different concrete mixes

Table 10 EDX test results for different concrete mixes showing elemental weights

Mix ID	EDX results	Elements								
		C	O	Na	Mg	Al	Si	Ca	Fe	
RM00	wt%	8.25	42.99	2.79	3.54	3.60	16.00	15.96	6.84	
	at. %	14.11	55.23	2.49	3.00	2.75	11.71	8.18	2.52	
RM05	wt%	3.63	36.84	2.18	3.20	4.79	19.50	14.96	10.09	
	at. %	5.95	46.89	1.95	2.86	4.21	15.27	5.67	5.92	
RM10	wt%	7.18	47.53	2.89	1.23	4.16	13.52	17.87	4.39	
	at. %	9.28	58.05	1.58	1.04	5.47	9.89	9.16	5.51	
RM15	wt%	8.62	44.46	2.27	1.94	4.31	17.78	13.44	5.00	
	at. %	12.75	55.10	1.03	1.64	4.52	12.01	7.89	3.84	
RM20	wt%	1.41	50.41	3.11	3.49	4.61	16.32	13.24	6.88	
	at. %	2.42	54.74	2.78	2.95	4.51	11.94	6.79	2.53	
RM25	wt%	10.42	42.29	2.91	1.04	4.60	16.11	10.06	10.35	
	at. %	17.82	52.32	2.60	0.88	4.50	10.79	5.16	3.81	

RM25), a gradual reduction at the elemental intensity of levels Ca, Si, and O can be noticed.

X-Ray Diffraction (XRD): A microstructural Test Results Interpretation

The XRD analysis of the concrete sample was carried out as in “X-ray Diffraction (XRD) Analysis: A Microstructural Test” Section to identify the presence of mineral phases and hydration products. The test was performed on the hardened concrete samples at the age of 28 days of curing. The crystalline phases present in the cement mortar are observed at different intensities (counts). The X-ray diffractogram shows different crystalline phases formed due to the hydration process. The patterns of the X-ray analysis are shown in Fig. 9.

The major peaks are identified by naming them numerically from 1 to 8. The crystalline mineral peaks present in the control concrete are more than the blended RM concrete peaks. The RM-blended concrete has a complex hydration process and exhibits multiple peaks of hydration products. The hydration products such as $\text{Ca}(\text{OH})_2$ and C–S–H are also observed. The XRD pattern of only cement mortar paste shows the presence of other crystalline materials such as quartz (SiO_2), calcite (CaCO_3), an-hydrated tri-calcium silicate (C_3S), and some ettringite phases.

A variation in the XRD patterns can be observed with an increase in the RM content. As RM has some pozzolanic properties, it reacts with $\text{Ca}(\text{OH})_2$, which is less than the amount produced due to the clinker’s hydration. It is observed that with the increase in the RM content, the quartz quantity increases in the mix. The formation of the ettringite is accelerated with the RM mixing. The portlandite quantity gradually decreases with the increase in the RM proportion. A small C–S–H phase variation is noticed. The C–S–H peaks beyond 15% RM reduce, and a slightly high peak of silica along with ettringite can be detected (Fig. 9; RM20,

RM25). At 10% and 15% RM replacement, a sharp peak can be observed due to the presence of a large amount of ettringite. At 25% replacement (RM25), small peaks are detected representing quartz, ettringite, gehlenite ($\text{Ca}_2\text{Al}(\text{AlSiO}_2)$), and small peaks of C–S–H gel. This discussion on XRD justifies RM15 as a better blend than other mixes.

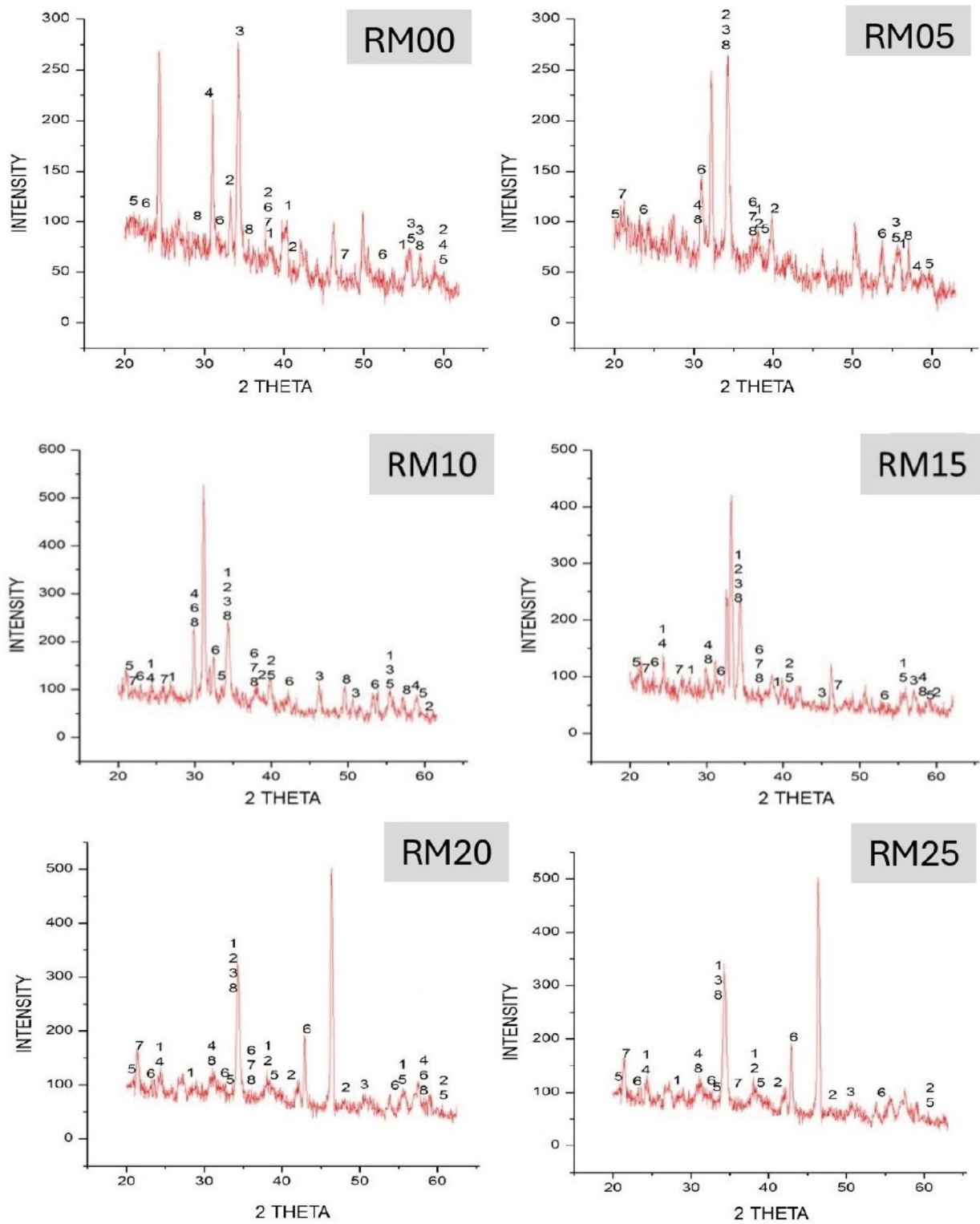
Critical Discussions on Microstructural Analysis

The microstructural analysis explains the morphology, elemental percentage, and crystallinity in the concrete mixes. The primary purpose of this microstructural analysis is to establish the superior RM-blended mix among all five blends. It is thus established that the blended concrete with RM 15% replacement level is the preferred one among the series owing to compact crystalline structures confirming C–S–H gel availability, solid form of CH phase, balanced content of alumina, silica, Fe traces, larger C–S–H and silica peaks justifying its larger mechanical characteristics.

Conclusion

In the current manuscript, a process of developing sustainable concrete is intended by replacing cement with RM at different proportions to find the most preferred replacement level through various fresh and hardened concrete characteristics. The following conclusions can be derived based on the detailed characteristics tests:

- The optimal RM replacement level is established to be 15% from the fresh characteristics study. However, the workability varies inversely, and the concrete density changes directly with the increase in the RM replacement level.



1- C_2S 3- Calcite 5- Portlandite 7- Ettringite
 2- C_3S 4- Quartz 6- Wollastonite 8- CSH

Fig. 9 XRD test results for different concrete mixes

- Though the concrete quality of the control mix is similar to that of RM-blended mixes up to 15% replacement, from remaining mechanical characterization tests, it can be concluded that RM15 is the optimal blended mix, providing maximum mechanical strength among all blended mixes and having acceptable strength reduction concerning the control mix. The NDT-RH test results lie within $\pm 25\%$ of the DT-CS results.
- In RM-blended mixes, a larger strength reduction rate is noticed at a higher curing period.
- All durability test results are conclusive on the fact that the RM-blended mixes are more durable than conventional concrete.
- The optimal RM replacement level is evaluated to be 15% from the acid resistance test. However, on enhancing the RM replacement level beyond 15%, the RM-blended concrete becomes more resistant in both sulfate and chloride resistance tests. But beyond 15% RM replacement, strength reduction is substantial. Thus, the optimal RM replacement level is declared to be 15% from the durability characteristics study.
- The blended concrete with RM 15% replacement level is the preferred one among the series owing to compact crystalline structures confirming C–S–H gel availability, solid form of CH phase, balanced content of alumina, silica, Fe traces, larger C–S–H and silica peaks justifying its larger mechanical characteristics.
- Thus, from the detailed fresh and hardened concrete characteristics study, the optimal red mud replacement level is evaluated to be 15%, promoting effective waste management.

Scope for Future Studies

- The structural behavior of the optimized mix, i.e., 85% OPC and 15% RM, must be studied.
- Cost analysis of the mix must be taken care of as this enhances sustainability.
- Other different SCMs should be investigated, and optimized composition must be identified.

Supplementary Information The online version contains supplementary material available at <https://doi.org/10.1007/s40831-024-00837-y>.

Acknowledgements The authors duly acknowledge the support received from Mr. Sukanta Sahu, SIKKA India Pvt Ltd, Mumbai, toward the supply of plasticizers in the present work.

Declarations

Competing Interests The authors declare that they have no known competing financial interests or personal relationships that could have appeared to influence the work reported in this paper.

Ethical Approval This research did not involve human participants and/or animals performed by any of the authors.

References

1. Piro NS, Mohammed AS, Hamad SM (2023) Evaluate and predict the resist electric current and compressive strength of concrete modified with ggbs and steelmaking slag using mathematical models. *J Sustain Metall* 9:194–215. <https://doi.org/10.1007/s40831-022-00631-8>
2. Das R, Panda S, Saumendra Sahoo A, Kumar Panigrahi S (2023) Effect of superplasticizer types and dosage on the flow characteristics of GGBFS based self-compacting geopolymer concrete. *Mater Today Proc*. <https://doi.org/10.1016/j.matpr.2023.06.339>
3. Li VC (2019) High-performance and multifunctional cement-based composite material. *Engineering* 5:250–260. <https://doi.org/10.1016/j.eng.2018.11.031>
4. Das SK, Rajput P, Mustakim SM, Bhoi B (2023) Towards sustainable construction: utilization of ferrochrome slag as Portland cement replacement in cementitious composites. *J Sustain Metall* 9:329–340. <https://doi.org/10.1007/s40831-023-00653-w>
5. Parhi SK, Panda S, Dwibedy S, Panigrahi SK (2024) Metaheuristic optimization of machine learning models for strength prediction of high-performance self-compacting alkali-activated slag concrete. *Multiscale Multidiscip Model Exp Des*. <https://doi.org/10.1007/s41939-023-00349-4>
6. Tang WC, Wang Z, Liu Y, Cui HZ (2018) Influence of red mud on fresh and hardened properties of self-compacting concrete. *Constr Build Mater* 178:288–300. <https://doi.org/10.1016/j.conbuildmat.2018.05.171>
7. Vavouraki AI (2020) Utilization of industrial waste slags to enhance ground waste concrete-based inorganic polymers. *J Sustain Metall* 6:383–399. <https://doi.org/10.1007/s40831-020-00281-8>
8. Liapis A, Anastasiou EK, Papachristoforou M, Papayianni I (2018) Feasibility study and criteria for eaf slag utilization in concrete products. *J Sustain Metall* 4:68–76. <https://doi.org/10.1007/s40831-017-0152-2>
9. Pradhan J, Panda S, Dwibedy S et al (2023) Production of durable high-strength self-compacting geopolymer concrete with GGBFS as a precursor. *J Mater Cycles Waste Manag* 26(1):529–551
10. Lothenbach B, Scrivener K, Hooton RD (2011) Supplementary cementitious materials. *Cem Concr Res* 41:1244–1256
11. Juenger MC, Snellings R, Bernal SA (2019) Supplementary cementitious materials: new sources, characterization, and performance insights. *Cem Concr Res* 122:257–273
12. Subedi S, Arce GA, Hassan MM et al (2022) Evaluation of alternative sources of supplementary cementitious materials for concrete materials. *Transp Res Rec* 2676:287–301
13. Pradhan J, Panda S, Kumar Mandal R, Kumar Panigrahi S (2023) Influence of GGBFS-based blended precursor on fresh properties of self-compacting geopolymer concrete under ambient temperature. *Mater Today Proc*. <https://doi.org/10.1016/j.matpr.2023.06.338>
14. Pradhan P, Panda S, Parhi SK, Panigrahi SK (2022) Factors affecting production and properties of self-compacting geopolymer concrete—a review. *Constr Build Mater* 344:128174
15. Liu X, Zhang N (2011) Utilization of red mud in cement production: a review. *Waste Manag Res J Sustain Circ Econ* 29:1053–1063. <https://doi.org/10.1177/0734242X11407653>
16. Anirudh M, Rekha KS, Venkatesh C, Nerella R (2021) Characterization of red mud based cement mortar; mechanical and microstructure studies. *Mater Today Proc* 43:1587–1591

17. Rathod RR, Suryawanshi NT, Memade PD (2013) Evaluation of the properties of red mud concrete. *IOSR J Mech Civil Eng* 1:31–34
18. Sawant AB, Kumthekar MB, Diwan VV, Hiraskar KG (2012) Experimental study on partial replacement of cement by neutralized red mud in concrete. *Int J Eng Adv Technol* 2:282–286
19. Liu X, Zhang N (2011) Utilization of red mud in cement production: a review. *Waste Manag Res* 29:1053–1063
20. Ribeiro DV, Labrincha JA, Morelli MR (2011) Potential use of natural red mud as pozzolan for Portland cement. *Mater Res* 14:60–66
21. Tsakiridis PE, Agatzini-Leonardou S, Oustadakis P (2004) Red mud addition in the raw meal for the production of Portland cement clinker. *J Hazard Mater* 116:103–110
22. Saravanan B, Vijayan DS (2020) Status review on experimental investigation on replacement of red-mud in cementitious concrete. *Mater Today Proc* 33:593–598
23. Putrevu M, Thiagarajan JS, Pasla D et al (2021) Valorization of red mud waste for cleaner production of construction materials. *J Hazard Toxic Radioact Waste* 25:03121002. [https://doi.org/10.1061/\(ASCE\)HZ.2153-5515.0000629](https://doi.org/10.1061/(ASCE)HZ.2153-5515.0000629)
24. Yan P, Chen B, Haque MA, Liu T (2023) Influence of red mud on the engineering and microstructural properties of sustainable ultra-high performance concrete. *Constr Build Mater* 396:132404
25. IS 8112 (1989) Specification for 43 grade ordinary Portland cement
26. Pradhan J, Panda S, Parhi SK et al (2024) GGBFS-based self-compacting geopolymer concrete with optimized mix parameters established on fresh, mechanical, and durability characteristics. *J Mater Civ Eng* 36:04023578. <https://doi.org/10.1061/JMCEE7.MTENG-16669>
27. IS 2386-1 (1963) Methods of test for aggregates for concrete, Part 1: particle size and shape
28. IS 2386-3 (1963) Methods of test for aggregates for concrete, Part 3: specific gravity, density, voids, absorption and bulking
29. IS 4031-11 (1988) Methods of physical tests for hydraulic cement, Part 11: Determination of density
30. IS 4031-2 (1999) Methods of physical tests for hydraulic cement, Part 2: Determination of fineness by specific surface by blaine air permeability method
31. IS 4031-4 (1988) Methods of physical tests for hydraulic cement, Part 4: Determination of consistency of standard cement paste
32. IS 4031-5 (1988) Methods of physical tests for hydraulic cement, Part 5: Determination of initial and final setting times
33. IS 10262 (2009) Guidelines for concrete mix design proportioning
34. Kumar BR, Ramakrishna G (2023) Performance evaluation of red mud as a construction material—a review. *Mater Today Proc*. <https://doi.org/10.1016/j.matpr.2023.04.043>
35. Venkatesh C, Chand MSR, Nerella R (2019) A state of the art on red mud as a substitutional cementitious material. *Annales de Chimie: Sci des Materiaux* 43:99–103
36. Panigrahi SK, Deb A, Bhattacharyya SK (2016) Modes of failure in shear deficient RC T-beams strengthened with FRP. *J Compos Constr* 20:04015029. [https://doi.org/10.1061/\(ASCE\)CC.1943-5614.0000586](https://doi.org/10.1061/(ASCE)CC.1943-5614.0000586)
37. Pradhan P, Panda S, Parhi SK, Panigrahi SK (2022) Effect of critical parameters on the fresh properties of self compacting geopolymer concrete. *Mater Today Proc* 62:6325–6335
38. IS 1199 (1959) Methods of sampling and analysis of concrete
39. SP 23 (1982) Handbook on concrete mixes
40. Pradhan P, Panda S, Parhi SK, Panigrahi SK (2022) Variation in fresh and mechanical properties of GGBFS based self-compacting geopolymer concrete in the presence of NCA and RCA. *Mater Today Proc* 62:6348–6358
41. IS 13311-1 (1992) Method of non-destructive testing of concrete, Part 1: Ultrasonic pulse velocity
42. IS 13311-2 (1992) Method of non-destructive testing of concrete-methods of test, Part 2: rebound hammer
43. Panigrahi SK, Deb A, Bhattacharyya SK (2015) Effect of laminate stiffness on failure mode in FRP wrapped T beams. *IJRET* 4:510–520
44. IS 516 (1959) Method of tests for strength of concrete
45. IS 5816 (1999) Method of test splitting tensile strength of concrete
46. Panigrahi SK, Sahoo AK (2003) Possible use of T-section columns in RC frame. *Indian Concr J* 77:1518–1522
47. Pradhan P, Dwibedy S, Pradhan M et al (2022) Durability characteristics of geopolymer concrete-progress and perspectives. *J Build Eng*. <https://doi.org/10.1016/j.jobe.2022.105100>
48. Fernandes I, Pericão M, Hagelia P et al (2012) Identification of acid attack on concrete of a sewage system. *Mater Struct* 45:337–350. <https://doi.org/10.1617/s11527-011-9769-y>
49. ASTM C 1898 (2020) Standard test methods for determining the chemical resistance of concrete products to acid attack
50. Marchand J, Odler I, Skalny JP (2001) Sulfate attack on concrete. CRC Press, Boca Raton
51. ASTM C 1218 (2020) Standard test method for water-soluble chloride in mortar and Concrete
52. ASTM C 1723 (2016) Standard guide for examination of hardened concrete using scanning electron microscopy
53. ASTM E 1508-12a 2019 Standard guide for quantitative analysis by energy-dispersive spectroscopy
54. ASTM C 1365 (2018) Standard test method for determination of the proportion of phases in Portland cement and Portland-cement clinker using x-ray powder diffraction analysis
55. Parhi SK, Dwibedy S, Panda S, Panigrahi SK (2023) A comprehensive study on controlled low strength material. *J Build Eng*. <https://doi.org/10.1016/j.jobe.2023.107086>
56. Wang Z, Pu L, Yao Y et al (2023) Unveiling the role of reactive magnesia and red mud in CO₂-cured aerated concrete. *J Build Eng* 78:107704
57. Wu P, Liu X, Zhang Z et al (2023) The harmless and value-added utilization of red mud: recovering iron from red mud by pyrometallurgy and preparing cementitious materials with its tailings. *J Ind Eng Chem*. <https://doi.org/10.1016/j.jiec.2023.11.038>
58. Tang R, Zhao B, Tian C et al (2023) Preliminary study of pre-heated decarburized activated coal gangue-based cemented paste backfill material. *Materials* 16:2354
59. Patangia J, Saravanan TJ, Kabeer KSA, Bisht K (2023) Study on the utilization of red mud (bauxite waste) as a supplementary cementitious material: pathway to attaining sustainable development goals. *Constr Build Mater* 375:131005
60. Chen S, Ou X, Jiang J, Tan Z (2023) Experimental Study on the curing mechanism of red mud-based stabilized soil co-modified by Nano-SiO₂ and gypsum. *Materials* 16:6016
61. Elahi MMA, Shearer CR, Reza ANR et al (2021) Improving the sulfate attack resistance of concrete by using supplementary cementitious materials (SCMs): a review. *Constr Build Mater* 281:122628

Publisher's Note Springer Nature remains neutral with regard to jurisdictional claims in published maps and institutional affiliations.

Springer Nature or its licensor (e.g. a society or other partner) holds exclusive rights to this article under a publishing agreement with the author(s) or other rightsholder(s); author self-archiving of the accepted manuscript version of this article is solely governed by the terms of such publishing agreement and applicable law.